Title
Innervation of pathologies in the lumbar vertebral end plate and intervertebral disc

Journal
The Spine Journal, 14(3)

ISSN
1529-9430

Authors
Fields, Aaron J
Liebenberg, Ellen C
Lotz, Jeffrey C

Publication Date
2014-03-01

DOI
10.1016/j.spinee.2013.06.075

Peer reviewed

Published in final edited form as:
Spine J. 2014 March 1; 14(3): 513–521. doi:10.1016/j.spinee.2013.06.075.

Innervation of pathologies in the lumbar vertebral endplate and intervertebral disc

Aaron J. Fields, Ph.D., **Ellen C. Liebenberg, B.S.**, and **Jeffrey C. Lotz, Ph.D.**
Orthopaedic Bioengineering Laboratory, Department of Orthopaedic Surgery, University of California, San Francisco, CA, United States

Introduction

Chronic low back pain (CLBP) is a spinal condition with a substantial socioeconomic burden [1]. Magnetic resonance imaging (MRI) is a powerful diagnostic tool for many spinal conditions, but MRI findings have limited diagnostic value for CLBP because of the unclear relationship between any anatomic abnormalities seen on MRI and symptoms reported by the patient [2–4]. Although symptoms can have many causes [5], one important cause is thought to be the presence of innervated pathologies of the vertebral endplate and intervertebral disc, since nerves in these pathologies may become sensitized by chemical [6] or mechanical [7] stimuli. Assessing the innervation of endplate and disc pathologies — and determining the relationship between these pathologies and any abnormalities seen on MRI — may therefore clarify the tissue sources of back pain and help to identify abnormalities with enhanced diagnostic value.

Innervated pathologies of the endplate and disc are thought to underlie many cases of chronic low back pain. In symptomatic patients, innervation is greater in endplates with cartilage and subchondral bone damage [8, 9], perhaps as a chemotactic response to neurotrophin production by disc cells [10] and new blood vessels [11]. Innervation is also greater in painful discs with annulus fissures [12, 13], which may provide a chemically and mechanically favorable environment for perivascular nerve growth [12, 14]. While these findings suggest that endplate damage and internal disc disruption can cause pain, the diagnostic value of these observations is limited because it is unknown how endplate and disc pathologies are innervated in general, and whether MRI is capable of detecting features that associate with neoinnervation. Thus, we sought to quantify innervation in the vertebral endplate and intervertebral disc, and to relate variation in innervation to the presence of pathologic features observed by histology and conventional MRI.

Please address all correspondence and reprint requests to: Jeffrey C. Lotz, Ph.D., 513 Parnassus Avenue, S-1157, University of California, San Francisco, CA 94143-0514, United States, (415) 476-7881, fax (415) 476-1128, lotzj@orthosurg.ucsf.edu.

Conflicts of Interest:
Jeffrey Lotz is a consultant for Relievant Medsystems who provided partial support for this study

Methods

Cadaver materials and MRI

Ninety-two vertebral endplates (from T11 to S1) and 46 corresponding intervertebral discs (from T11/T12 to L5/S1) were obtained from seven human thoracolumbar spines (donor ages 51–67 years; two females and five males). All spines were scanned *in-situ* using MRI (GE 3T Signa HDx scanner; GE Healthcare, Waukesha, WI) with sagittal T1- and T2-weighted fast spin-echo sequences. The T1-weighted sequence comprised the following: TE 15.6 ms, TR 516 ms, echo train length 2, acquisition matrix 256 × 256, slice thickness 3 mm. The T2-weighted sequence comprised the following: TE 61.6 ms, TR 2500 ms, echo train length 8, acquisition matrix 256 × 256, slice thickness 3 mm.

Endplate and disc abnormalities on MRI

After scanning the spines, we rated the images for endplate and disc abnormalities using established criteria. Endplate signal intensity changes, or Modic changes [15], are related to pathologies of the endplate and bone marrow, and have two main types: Type 1 changes are hypointense on T1-weighted images and hyperintense on T2-weighted images, and Type 2 changes are hyperintense on T1-weighted images and either iso- or hyperintense on T2-weighted images. Both types of Modic changes collocate with endplate damage on histology, but Type 1 changes reflect fibrovascular replacement of the normal marrow elements, whereas Type 2 changes reflect fatty replacement of the marrow elements [15]. Two raters classified the endplates as ‘normal’, ‘Modic Type 1’, or ‘Modic Type 2’ (inter-rater reliability, $\kappa = 0.89$).

For the disc, we rated the MR images for high-intensity zones (HIZ), which are related to internal disc disruption. HIZ appear more hyperintense on T2-weighted images than does the adjacent nucleus pulposus [16, 17], and are thought to reflect neovascularized granulation tissue that occurs secondary to an annulus tear [18]. Two raters classified the discs as ‘normal’, ‘low-intensity’, or ‘high-intensity’ (inter-rater reliability, $\kappa = 0.67$). Also, we assessed disc degeneration using the Pfirrmann grading scheme [19] (inter-rater reliability, $\kappa = 0.74$).

Histology

Complete bone-disc-bone motion segments were prepared from the intact spines and processed for histology. First, the surrounding musculature and posterior elements were removed from the spines. Next, the spines were cut into four, 5–7 mm-thick para-sagittal slabs. One medial slab was chosen at random from each spine, and was fixed in formalin, radiographed, and then decalcified in a mild ion-exchange decalcifying agent (IED; Biocare Medical, Concord, CA). Radiographic assessment was used to monitor the decalcification process, which typically required 1 week to complete. After decalcification, the slabs were cut transversely to produce motion segments containing one half of the cranial vertebral body, the intervertebral disc, and one half of the caudal vertebral body.

The resulting bone-disc-bone motion segments were processed for paraffin histology. Segments were first dehydrated in ethanol baths of ascending concentration, cleared in Clearite, and then infiltrated with paraffin. Next, 7-μm thick sections were cut from the blocks using a microtome (Microm 355 S; Thermo Fisher Scientific, Waltham, MA), mounted on slides, and stained with Heidenhain connective tissue stain that contains aniline blue, orange G and acid fuchsin. Adjacent slides were immuno-stained for the general neuronal marker protein gene product 9.5 (PGP 9.5; AbD Serotec, Kidlingdon, United Kingdom) using a polymer detection system (MACH 4 HRP; Biocare Medical, Concord, CA). PGP 9.5 is a cytoplasmic C-terminal hydrolase present in all classes of nerves and is

often used as a marker for spinal nerves [20, 21]. Compared to calcitonin gene-related protein and neurofilament 200, we found that staining for PGP 9.5 provides a high specificity for nerve tissue without confounding the background staining [20].

Histology grading

The motion segments were divided into sub-regions (Figure 1A), and each sub-region was rated for the presence and size of pathologic features of the vertebral endplates and the intervertebral disc. Pathologic features included the following:

1. Fibrovascular endplate marrow at the junction between the endplate and the disc (Figure 1B) was defined according to the original description [15] as fibrous tissue within marrow space devoid of normal hematopoietic elements. Fibrovascular marrow was rated by its size relative to the area of the sub-region where it was observed: ‘absent’; ‘mild’, < 25% of sub-region; ‘moderate’, 25–50% of sub-region; and, ‘severe’, > 50% of sub-region.
2. Fatty endplate marrow at the junction between the endplate and the disc (Figure 1C) showed a decrease in hematopoietic cells and an increase in adipocytes compared to adjacent, normal marrow elements [15, 22]. The fatty marrow was rated by its size relative to the area of the subregion where it was observed: ‘absent’; ‘mild’, < 25% of sub-region; ‘moderate’, 25–50% of subregion; and, ‘severe’, > 50% of sub-region.
3. Endplate structural defects, or lesions, were identified using the criteria of Wang *et al.* [23]. These defects included endplate cartilage erosions and avulsions with exposed trabecular bone at the junction of the inner annulus and nucleus pulposus (Figure 1D), nodule-like indentations (Figure 1E), and fractures with exposed trabecular bone (Figure 1F). Endplate defects were rated by their overall size: ‘absent’; ‘small’, < 10 mm^2; ‘moderate’, 10–20 mm^2; and, ‘severe’, > 20 mm^2. If more than one defect was present, the largest defect was rated.
4. Annulus tears included concentric delamination and radial fissuring [24, 25], and were distinguishable from sectioning artifacts by the in-growth of tissue. Concentric tears (Figure 1G) were rated as follows: ‘absent’; ‘mild’, does not extend into endplate cartilage; ‘moderate’, extends into endplate cartilage; and, ‘severe’, extends through endplate cartilage. Radial tears (Figure 1H) were rated as follows: ‘absent’; ‘mild’, extends into inner annulus; ‘moderate’, extends into mid-annulus; and, ‘severe’, extends into outer annulus. If more than one of either type of tear was present, the most severe was rated.

Innervation

Nerve fibers positive for PGP 9.5 were counted in 10X fields-of-view (FOV) spanning each subregion of the motion segments, and were expressed in units of nerves/mm^2. If a sub-region contained endplate or disc pathologies, nerves were counted separately for FOV with and without pathologies. If two or more pathologies were present in an endplate, the total nerve density was calculated by dividing the total number of nerves by the area of all pathologies. Nerves were excluded if they occurred in the longitudinal ligaments.

Statistical analysis

We used Mann-Whitney U and Kruskal-Wallis tests to compare nerve density between pairs of groups and multiple groups, respectively. Descriptive statistics were used to compare the incidence of different endplate and disc pathologies, and to relate the incidence of pathologies on histology to their incidence on MRI. Statistical analyses were performed

using JMP (Version 10.0; SAS Institute, Cary, NC). All statistical tests were taken as significant at $p < 0.05$.

Results

Incidence and distribution of nerves

Nerves were observed in 82.6% (76) of the 92 vertebral endplates and were encountered in similar densities within the various anatomical regions. Nerve density was similar between cranial and caudal endplates (Figure 2A); nerve density was also similar among anterior, central, and posterior regions (Figure 2B). In general, nerve density ranged from 0–0.05 nerves/mm^2 and followed a non-normal distribution. On histology, these PGP 9.5-positive nerves often accompanied blood vessels that branched toward the endplates from the central vertebral body. These nerves were observed within and adjacent to the blood vessel walls (Figure 3A).

In the disc, nerves were observed in 30.4% (14) of the 46 levels and were highly localized to discrete bundles within the outer third of the annulus fibrosus. On histology, these PGP 9.5-positive nerves were sparsely distributed within the outermost layers of the annulus (Figure 3E). The absence of lumen, red blood cells, and vessel walls on the adjacent trichrome slides suggests that nerves in the disc were unassociated with blood vessels.

Incidence, distribution, and severity of pathologies

Overall, 42.3% (39) of the 92 endplates had at least one pathology; 7.6% (7) had multiple pathologies of the same type. Endplate defects (32.6%) were the most common pathology, and many endplates had more than one type of pathology. For example, 76.6% of endplates with defects were accompanied by abnormal marrow elements (Figure 1D, Figure 4). Endplate pathologies were more common in the anterior region than in either the central or posterior regions (Table 1). Fisher's exact tests indicated that the probabilities of fibrovascular marrow ($p = 0.06$), fatty marrow ($p = 0.001$), and endplate defects ($p < 0.0001$) were significantly associated with disc Pfirrmann grade.

Of the 46 intervertebral discs, 56.5% (26) had an annulus tear (Table 1). The incidence of concentric tears (39.1%) was similar to that for radial tears (34.7%), and several discs (17.4%) had both concentric and radial tears.

Innervation of pathologies of the endplate and disc

Nerves were observed in the majority of endplate pathologies and occurred at higher densities than did nerves in endplates without pathologies. Fibrovascular endplate marrow had significantly greater nerve density than did normal endplate marrow (Figure 5A). Because fibrovascular and fatty endplate marrow co-located with endplate defects (Figure 3D, Figure 4), nerve density was significantly higher in endplates with defects than in endplates without defects (Figure 5B). Nerves were present in 90% (27/30) of endplate defects, 88.8% (16/18) of fibrovascular endplate marrow, and 66.6% (14/21) of fatty endplate marrow. Nerves were observed in 66.1% (35/53) of endplates with no defects or abnormal marrow elements.

Nerves were observed in 34.6% (9/26) of the discs with annulus tears, and discs with radial tears in particular tended to be more innervated in terms of incidence and degree. For example, nerves were observed in 43.8% (7/16) of discs with radial tears, and the number of nerves observed in discs with radial tears tended to be greater than that in discs with no tears (Figure 6). By comparison, nerves were observed in 27.8% (5/18) of discs with concentric tears, and the number of nerves observed in discs with concentric tears was similar to that in

discs with no tears. Surprisingly, the nerves observed in discs with tears did not generally coincide with the location of the tear (Figure 3F). Nerves were observed in 25% (5/20) of the discs with no tears.

Compared to the most innervated endplate pathologies, *i.e.* fibrovascular endplate marrow and endplate defects, discs with radial tears were significantly less innervated (Figure 7).

Relationship between innervation and pathology size

Nerve density did not associate with the size of the fibrovascular marrow region ($p = 0.15$), the size of the fatty marrow region ($p = 0.97$), or the size of the endplate defect ($p = 0.20$). Furthermore, there was no association between the number of nerve fibers and tear size for either concentric tears ($p = 0.75$) or radial tears ($p = 0.33$).

Relationship between pathologies on histology and abnormalities on MRI

The majority of pathologies on histology were not detected on MRI. Type 1 Modic changes were observed in 11.1% (2/18) of endplates with fibrovascular marrow, and Type 2 Modic changes were observed in 61.9% (13/21) of endplates with fatty marrow. For the disc, high-intensity zones on T2 MRI were observed in 12.5% (2/16) of the discs with radial tears.

Discussion

These results indicate that vertebral endplate pathologies are more innervated than intervertebral disc pathologies, both in terms of the incidence and extent of innervation. In the endplate, nerves were evenly distributed in the hematopoietic bone marrow contiguous with the endplate. However, in areas with structural defects or endplate lesions, the marrow was often fibrovascular or fatty, and in such areas we observed a significant aggregation of nerves. Moreover, innervation in these endplate defects was greater than in discs with radial tears. This finding is surprising given the prevailing view that internal disc disruption causes CLBP. To diagnose internal disc disruption, clinicians must inject a contrast agent during discography [26], as internal disruption is not well visualized on standard MRI [27]. However, no such enhancing technique is used for improving visualization of endplate pathologies, which were often undetectable on MRI in our study. This discrepancy could lead to clinical bias in the perception of association between MRI findings and patient symptoms. We conclude that improved visualization of endplate pathologies may enhance the diagnostic value of MRI for CLBP.

Pathologies of the endplate bone marrow, *i.e.* Modic changes, are one of the most specific predictors of CLBP [28–31], and our findings indicate that these marrow pathologies are densely innervated by nociceptive fibers. The precise etiology of these marrow pathologies is not well understood, but it appears to involve autoimmune and inflammatory reactions to toxic chemicals produced by the disc [6]. For example, repeated trauma to the disc increases production of inflammatory cytokines such as interleukin (IL)-1, IL-6, IL-8, and tumor necrosis factor (TNF)-α [32–35]. In particular, IL-1 secretion by nucleus pulposus cells may stimulate the expression of angiogenic and neurotrophic factors [36], the latter of which can trigger nociceptive nerve ingrowth into the endplates [11]. A predisposing factor for the inflammatory reaction may be structural defects in the endplate cartilage and bone that enhance communication between the inflammatogenic nucleus and the vertebral bone marrow. In support of this notion, innervated marrow pathologies collocated with over 75% of the avulsion-, fracture-, and node-like endplate defects. This could also explain why those same types of endplate defects were highly predictive of back pain history in a recent study [37], and together, these findings underscore the relevance of neoinnervation and the clinical significance of endplate defects in CLBP.

Annulus high-intensity zones (HIZ) are also highly specific predictors of CLBP [16, 18, 26, 38], yet the underlying source of the pain is unclear. Inflammation and neoinnervation at the periphery of a radial tear is one potential source, as others have reported ingrowth of vascularized granulation tissue along fissures [13]. Yet, we observed nerves in only 35% of the discs with radial tears, and of the innervated cases, the location of the nerves did not actually coincide with the tear. One possible explanation for this finding is that nerve ingrowth into the disc is resisted by intradiscal pressure, proteoglycan content, and tissue impermeability [14]. Hence, although we observed radial fissures in this study comprising of discs with moderate stages of degeneration (Pfirrmann Grades 2–4), fissures may only support nerve ingrowth in discs with extreme degeneration (Pfirrmann Grade 5). Alternatively, the pain source in some patients with disc pathologies could be nerves in the adjacent endplate rather than in the disc. Of the discs with radial tears in the current study, 63% bordered at least one defected endplate, and endplate defects were more frequently innervated — and to a greater degree — than were radial tears. Consistent with this view, Hsu *et al.* report that the probability of reproducing patient symptoms during discography was significantly greater in cases with endplate damage [39]. Hence, the existence of highly innervated endplate pathologies along with annulus tears makes it difficult to discern the pain source.

Many factors influence the diagnostic performance of MRI. Low inter-rater reliability for HIZ ($\kappa = 0.67$) reduced its diagnostic performance for identifying annulus tears. Had rater agreement been perfect in this study, HIZ would have been observed in 31.3% (5/16) of discs with radial tears, not 12.5% (2/16). Despite this improvement, MRI still misses many tears. However, given that so few tears were innervated, any potential clinical benefits of improving visualization of annulus tears on MRI — without consideration for innervation — are not obvious.

Similarly, we detected only a small fraction of the endplate pathologies on MRI. This is consistent with trends from cadaveric studies using MRI [40], radiography [41–43], and discography [42], and is especially noteworthy because our findings indicate that the majority of these endplate pathologies were highly innervated. These data also help explain observations that Modic changes, while quite specific, have only modest sensitivity for predicting discography-confirmed CLBP [5, 28, 29, 31, 44–46]. A key aspect of increasing MRI sensitivity, therefore, may be improving visualization of innervated endplate pathologies. For example, innervated fibrovascular and fatty marrow may be more apparent with fat suppression T2 sequences [47]. Also, since marrow abnormalities bordered endplate defects such as fractures (Figure 1F) and cartilage avulsions/erosions (Figures 1D, 3D, 4), this motivates the use of diagnostic techniques that improve endplate visualization, such as ultra-short time-to-echo (UTE) MRI sequences [48] or pharmacological enhancement of endplate diffusion [49].

The coexistence of endplate and annulus defects on histology, combined with the difficulty of visualizing these defects on MRI, could confound attempts to sub-classify CLBP patients for predictive or prognostic purposes. In particular, clinical studies involving 120 and 736 CLBP patients reported that Modic changes and HIZ rarely coexist [46, 50], which suggests that patients have distinct vertebrogenic or annulogenic pain phenotypes. However, our data indicate that the coexistence of Modic- and HIZ-like pathologies could be missed on MRI. Increasing MRI sensitivity could therefore clarify the relationship between endplate and annulus defects, including whether vertebrogenic or annulogenic phenotypes influence treatment outcomes.

This study had several unique features compared with previous studies that investigated endplate or disc innervation [12, 21, 51, 52]. Most notably, we mapped the spatial

distribution of nerves in endplate and disc pathologies from a modest number of spine segments, which enabled us to compare innervation amongst the different pathologies. We also related the incidence of histologic pathologies to abnormalities seen on MRI. This is beyond the capability of biopsy studies, wherein it can be difficult to obtain intact segments for histologic evaluation. A limitation of this study was that we evaluated only a few mid-sagittal slides per level, which could lead to underestimation of pathology incidence [24]. A second limitation was the lack of medical history, which prevents us from concluding that any of the observed defects were symptomatic. Nerve density alone is insufficient to infer symptoms, which depend also on nociceptor threshold, mechanical factors, and psychosocial influences [53]. The smallest nerve fibers in the endplate and disc were between 1–5 μm in diameter, which suggests they were either myelinated (A-δ) fibers that transmit sharp pain or large unmyelinated (C) fibers that transmit dull pain [53], although these types of nerves can serve other functions including temperature, pressure, or touch sensations. Nevertheless, the trend of increased innervation in endplate and disc pathologies correlates with findings in CLBP patients [8, 9, 12, 13], and is also consistent with the relationship between these types of endplate pathologies and back pain history [37], lending confidence to the clinical validity of our findings.

In summary, we determined that vertebral endplate pathologies are more innervated than intervertebral disc pathologies, both in terms of the incidence and degree of innervation. Additionally, we found that many innervated endplate pathologies were not detectable on MRI. MRI findings have limited diagnostic value for CLBP, in part because of the unclear relationship between anatomic abnormalities seen on MRI and symptoms reported by the patient. Taken together, our findings indicate that improved visualization of endplate pathologies may enhance the diagnostic value of MRI for CLBP.

Acknowledgments

Funding Sources: National Institutes of Health Grant AR052811 Relievant Medsystems

References

1. Katz JN. Lumbar disc disorders and low-back pain: socioeconomic factors and consequences. J Bone Joint Surg Am. 2006; 88 (Suppl 2):21–4. [PubMed: 16595438]
2. Boden SD, Davis DO, Dina TS, Patronas NJ, Wiesel SW. Abnormal magnetic-resonance scans of the lumbar spine in asymptomatic subjects. A prospective investigation. J Bone Joint Surg Am. 1990; 72(3):403–8. [PubMed: 2312537]
3. Sheehan NJ. Magnetic resonance imaging for low back pain: indications and limitations. Ann Rheum Dis. 2010; 69(1):7–11. [PubMed: 20007621]
4. Chou D, Samartzis D, Bellabarba C, et al. Degenerative magnetic resonance imaging changes in patients with chronic low back pain: a systematic review. Spine. 2011; 36(21 Suppl):S43–53. [PubMed: 21952189]
5. Carragee EJ, Alamin TF, Miller JL, Carragee JM. Discographic, MRI and psychosocial determinants of low back pain disability and remission: a prospective study in subjects with benign persistent back pain. Spine J. 2005; 5(1):24–35. [PubMed: 15653082]
6. Crock HV. Internal disc disruption. A challenge to disc prolapse fifty years on. Spine. 1986; 11(6): 650–3. [PubMed: 3787337]
7. Kuslich SD, Ulstrom CL, Michael CJ. The tissue origin of low back pain and sciatica: a report of pain response to tissue stimulation during operations on the lumbar spine using local anesthesia. Orthop Clin North Am. 1991; 22(2):181–7. [PubMed: 1826546]
8. Brown MF, Hukkanen MV, McCarthy ID, et al. Sensory and sympathetic innervation of the vertebral endplate in patients with degenerative disc disease. J Bone Joint Surg Br. 1997; 79(1): 147–53. [PubMed: 9020464]

9. Ohtori S, Inoue G, Ito T, et al. Tumor necrosis factor-immunoreactive cells and PGP 9.5-immunoreactive nerve fibers in vertebral endplates of patients with discogenic low back Pain and Modic Type 1 or Type 2 changes on MRI. Spine. 2006; 31(9):1026–31. [PubMed: 16641780]
10. Garcia-Cosamalon J, del Valle ME, Calavia MG, et al. Intervertebral disc, sensory nerves and neurotrophins: who is who in discogenic pain? J Anat. 2010; 217(1):1–15. [PubMed: 20456524]
11. Freemont AJ, Watkins A, Le Maitre C, et al. Nerve growth factor expression and innervation of the painful intervertebral disc. J Pathol. 2002; 197(3):286–92. [PubMed: 12115873]
12. Freemont AJ, Peacock TE, Goupille P, Hoyland JA, O'Brien J, Jayson MI. Nerve ingrowth into diseased intervertebral disc in chronic back pain. Lancet. 1997; 350(9072):178–81. [PubMed: 9250186]
13. Peng B, Wu W, Hou S, Li P, Zhang C, Yang Y. The pathogenesis of discogenic low back pain. J Bone Joint Surg Br. 2005; 87(1):62–7. [PubMed: 15686239]
14. Stefanakis M, Al-Abbasi M, Harding I, et al. Annulus Fissures are Mechanically and Chemically Conducive to the Ingrowth of Nerves and Blood Vessels. Spine. 2012
15. Modic MT, Steinberg PM, Ross JS, Masaryk TJ, Carter JR. Degenerative disk disease: assessment of changes in vertebral body marrow with MR imaging. Radiology. 1988; 166(1 Pt 1):193–9. [PubMed: 3336678]
16. Aprill C, Bogduk N. High-intensity zone: a diagnostic sign of painful lumbar disc on magnetic resonance imaging. Br J Radiol. 1992; 65(773):361–9. [PubMed: 1535257]
17. Vanharanta H, Sachs BL, Spivey MA, et al. The relationship of pain provocation to lumbar disc deterioration as seen by CT/discography. Spine. 1987; 12(3):295–8. [PubMed: 3589823]
18. Lam KS, Carlin D, Mulholland RC. Lumbar disc high-intensity zone: the value and significance of provocative discography in the determination of the discogenic pain source. Eur Spine J. 2000; 9(1):36–41. [PubMed: 10766075]
19. Pfirrmann CW, Metzdorf A, Zanetti M, Hodler J, Boos N. Magnetic resonance classification of lumbar intervertebral disc degeneration. Spine. 2001; 26(17):1873–8. [PubMed: 11568697]
20. Bailey JF, Liebenberg E, Degmetich S, Lotz JC. Innervation patterns of PGP 9.5-positive nerve fibers within the human lumbar vertebra. J Anat. 2011; 218(3):263–70. [PubMed: 21223256]
21. Fagan A, Moore R, Vernon Roberts B, Blumbergs P, Fraser R. ISSLS prize winner: The innervation of the intervertebral disc: a quantitative analysis. Spine. 2003; 28(23):2570–6. [PubMed: 14652473]
22. Elmore SA. Enhanced histopathology of the bone marrow. Toxicol Pathol. 2006; 34(5):666–86. [PubMed: 17067952]
23. Wang Y, Videman T, Battie MC. Lumbar vertebral endplate lesions: prevalence, classification, and association with age. Spine. 2012; 37(17):1432–9. [PubMed: 22333959]
24. Vernon-Roberts B, Moore RJ, Fraser RD. The natural history of age-related disc degeneration: the pathology and sequelae of tears. Spine. 2007; 32(25):2797–804. [PubMed: 18246000]
25. Boos N, Weissbach S, Rohrbach H, Weiler C, Spratt KF, Nerlich AG. Classification of age-related changes in lumbar intervertebral discs: 2002 Volvo Award in basic science. Spine. 2002; 27(23): 2631–44. [PubMed: 12461389]
26. Sachs BL, Vanharanta H, Spivey MA, et al. Dallas discogram description. A new classification of CT/discography in low-back disorders. Spine. 1987; 12(3):287–94. [PubMed: 2954226]
27. Zucherman J, Derby R, Hsu K, et al. Normal magnetic resonance imaging with abnormal discography. Spine. 1988; 13(12):1355–9. [PubMed: 2975063]
28. Braithwaite I, White J, Saifuddin A, Renton P, Taylor BA. Vertebral end-plate (Modic) changes on lumbar spine MRI: correlation with pain reproduction at lumbar discography. Eur Spine J. 1998; 7(5):363–8. [PubMed: 9840468]
29. Weishaupt D, Zanetti M, Hodler J, et al. Painful lumbar disk derangement: relevance of endplate abnormalities at MR imaging. Radiology. 2001; 218(2):420–7. [PubMed: 11161156]
30. Kjaer P, Leboeuf-Yde C, Korsholm L, Sorensen JS, Bendix T. Magnetic resonance imaging and low back pain in adults: a diagnostic imaging study of 40-year-old men and women. Spine. 2005; 30(10):1173–80. [PubMed: 15897832]

31. O'Neill C, Kurgansky M, Kaiser J, Lau W. Accuracy of MRI for diagnosis of discogenic pain. Pain Physician. 2008; 11(3):311–26. [PubMed: 18523502]
32. Ahn SH, Cho YW, Ahn MW, Jang SH, Sohn YK, Kim HS. mRNA expression of cytokines and chemokines in herniated lumbar intervertebral discs. Spine. 2002; 27(9):911–7. [PubMed: 11979160]
33. Burke JG, Watson RW, McCormack D, Dowling FE, Walsh MG, Fitzpatrick JM. Intervertebral discs which cause low back pain secrete high levels of proinflammatory mediators. J Bone Joint Surg Br. 2002; 84(2):196–201. [PubMed: 11924650]
34. Olmarker K, Larsson K. Tumor necrosis factor alpha and nucleus-pulposus-induced nerve root injury. Spine. 1998; 23(23):2538–44. [PubMed: 9854752]
35. Weiler C, Nerlich AG, Bachmeier BE, Boos N. Expression and distribution of tumor necrosis factor alpha in human lumbar intervertebral discs: a study in surgical specimen and autopsy controls. Spine. 2005; 30(1):44–53. discussion 4. [PubMed: 15626980]
36. Lee JM, Song JY, Baek M, et al. Interleukin-1beta induces angiogenesis and innervation in human intervertebral disc degeneration. J Orthop Res. 2011; 29(2):265–9. [PubMed: 20690185]
37. Wang Y, Videman T, Battie MC. ISSLS prize winner: Lumbar vertebral endplate lesions: associations with disc degeneration and back pain history. Spine. 2012; 37(17):1490–6. [PubMed: 22648031]
38. Ito M, Incorvaia KM, Yu SF, Fredrickson BE, Yuan HA, Rosenbaum AE. Predictive signs of discogenic lumbar pain on magnetic resonance imaging with discography correlation. Spine. 1998; 23(11):1252–8. discussion 9-60. [PubMed: 9636979]
39. Hsu KY, Zucherman JF, Derby R, White AH, Goldthwaite N, Wynne G. Painful lumbar endplate disruptions - a significant discographic finding. Spine. 1988; 13(1):76–8. [PubMed: 2967995]
40. Benneker LM, Heini PF, Anderson SE, Alini M, Ito K. Correlation of radiographic and MRI parameters to morphological and biochemical assessment of intervertebral disc degeneration. Eur Spine J. 2005; 14(1):27–35. [PubMed: 15723249]
41. Hilton RC, Ball J. Vertebral rim lesions in the dorsolumbar spine. Ann Rheum Dis. 1984; 43(2): 302–7. [PubMed: 6712302]
42. Malmivaara A, Videman T, Kuosma E, Troup JD. Plain radiographic, discographic, and direct observations of Schmorl's nodes in the thoracolumbar junctional region of the cadaveric spine. Spine. 1987; 12(5):453–7. [PubMed: 3629396]
43. Yoganandan N, Maiman DJ, Pintar F, et al. Microtrauma in the lumbar spine: a cause of low back pain. Neurosurgery. 1988; 23(2):162–8. [PubMed: 2972940]
44. Buttermann GR, Heithoff KB, Ogilvie JW, Transfeldt EE, Cohen M. Vertebral body MRI related to lumbar fusion results. Eur Spine J. 1997; 6(2):115–20. [PubMed: 9209879]
45. Sandhu HS, Sanchez-Caso LP, Parvataneni HK, Cammisa FP Jr, Girardi FP, Ghelman B. Association between findings of provocative discography and vertebral endplate signal changes as seen on MRI. J Spinal Disord. 2000; 13(5):438–43. [PubMed: 11052355]
46. Thompson KJ, Dagher AP, Eckel TS, Clark M, Reinig JW. Modic changes on MR images as studied with provocative diskography: clinical relevance--a retrospective study of 2457 disks. Radiology. 2009; 250(3):849–55. [PubMed: 19244050]
47. van Goethem, JW. Magnetic resonance imaging of the spine. In: Reimer, P.; Parizel, PM.; Meaney, JF.; Stichnoth, FA., editors. Clinical MR Imaging: A Practical Approach. Berlin: Springer; 2010. p. 197-223.
48. Bae WC, Statum S, Zhang Z, et al. Morphology of the cartilaginous endplates in human intervertebral disks with ultrashort echo time MR imaging. Radiology. 2013; 266(2):564–74. [PubMed: 23192776]
49. Rajasekaran S, Venkatadass K, Naresh Babu J, Ganesh K, Shetty AP. Pharmacological enhancement of disc diffusion and differentiation of healthy, ageing and degenerated discs: Results from in-vivo serial post-contrast MRI studies in 365 human lumbar discs. Eur Spine J. 2008; 17(5):626–43. [PubMed: 18357472]
50. Marshman LA, Metcalfe AV, Krishna M, Friesem T. Are high-intensity zones and Modic changes mutually exclusive in symptomatic lumbar degenerative discs? J Neurosurg Spine. 2010; 12(4): 351–6. [PubMed: 20367371]

51. Antonacci MD, Mody DR, Heggeness MH. Innervation of the human vertebral body: a histologic study. J Spinal Disord. 1998; 11(6):526–31. [PubMed: 9884299]

52. Buonocore M, Aloisi AM, Barbieri M, Gatti AM, Bonezzi C. Vertebral body innervation: Implications for pain. J Cell Physiol. 2010; 222(3):488–91. [PubMed: 20020509]

53. Cavanaugh JM, Ozaktay AC, Yamashita T, Avramov A, Getchell TV, King AI. Mechanisms of low back pain: a neurophysiologic and neuroanatomic study. Clin Orthop Relat Res. 1997; (335): 166–80. [PubMed: 9020216]

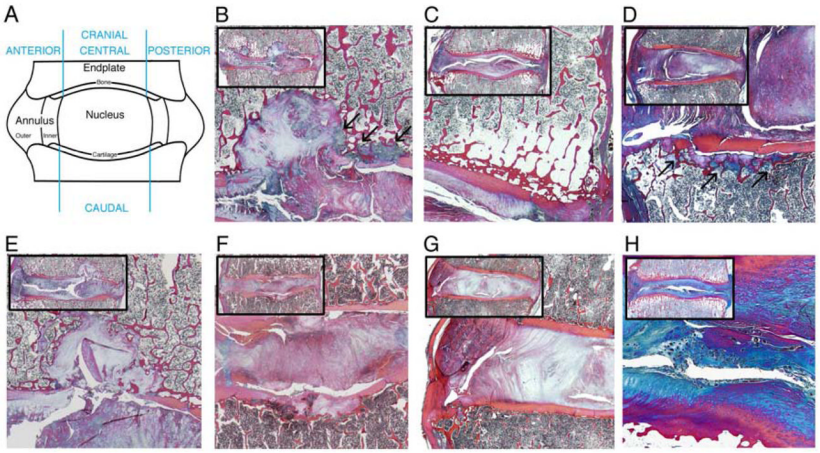

Figure 1.

Sub-regions of motion segments and various types of endplate and disc pathologies (see Methods for histological descriptions). **(A)** Sub-regions used to classify the location of endplate nerves and pathologies. **(B)** Fibrovascular endplate marrow. **(C)** Fatty endplate marrow. (**D)** Avulsion-type endplate defect. **(E)** Nodule-type endplate defect. **(F)** Fracture-type endplate defect. **(G)** Concentric annulus tear. **(H)** Radial annulus tear. Note: arrows indicate specified pathology in images where multiple pathologies are present; Heidenhain trichrome stain.

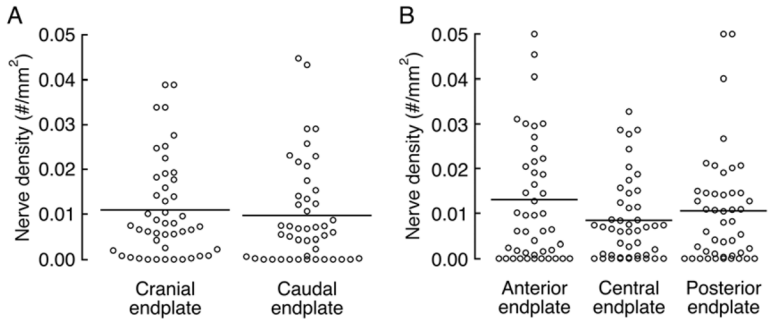

Figure 2.

Comparison of nerve density between cranial and caudal endplates and among anterior, central, and posterior regions. **(A)** Cranial and caudal endplates had similar nerve density ($p = 0.30$, Mann-Whitney U test). **(B)** Anterior, central, and posterior endplate regions had similar nerve density ($p = 0.60$, Kruskal-Wallis test). However, the nerve density in the anterior endplate region was significantly greater than that of the central endplate region when the nerve densities of the regions were compared pair-wise for each endplate ($p = 0.01$, Wilcoxon signed rank test). Note: data points in (B) represent the combined densities of cranial and caudal endplates for a given region. Horizontal lines indicate group means.

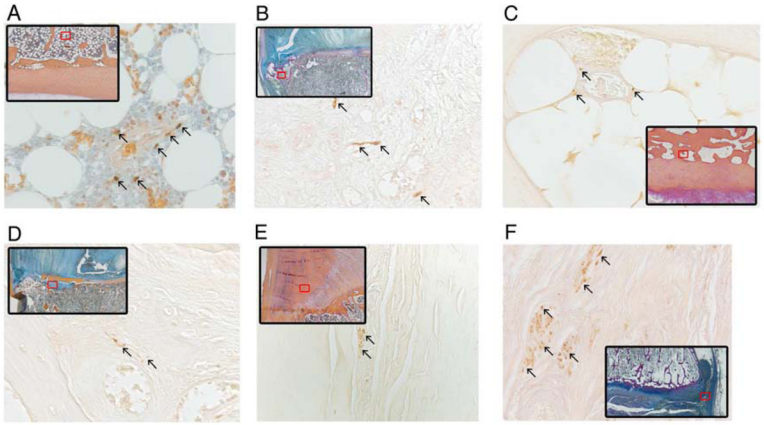

Figure 3.

Examples of PGP 9.5-positive nerves in the vertebral endplate and intervertebral disc. **(A)** Typical perivascular nerve in hematopoietic marrow adjacent to the endplate. **(B)** Nerves within fibrovascular endplate marrow. **(C)** Nerves within fatty endplate marrow. **(D)** Nerves in avulsion-type endplate defect. **(E)** Typical nerves in outer annulus of the disc. **(F)** Nerves in the outer annulus of a disc with a radial tear. Note: red box indicates location of high-magnification region of interest; arrows indicate PGP 9.5-positive nerve fibers.

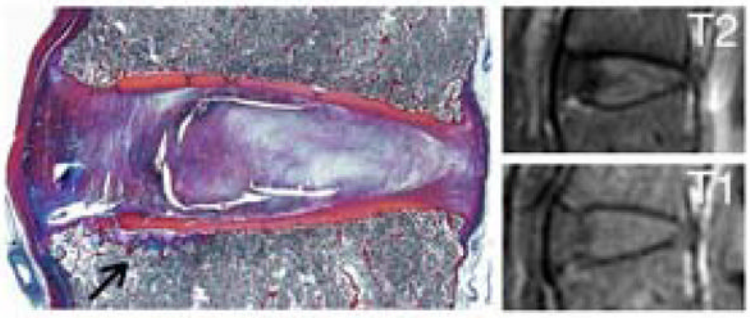

Figure 4.
Endplate cartilage avulsion with fibrovascular marrow (left) and corresponding MR images (right). Donor information: 63-year-old woman; L3–L4 disc.

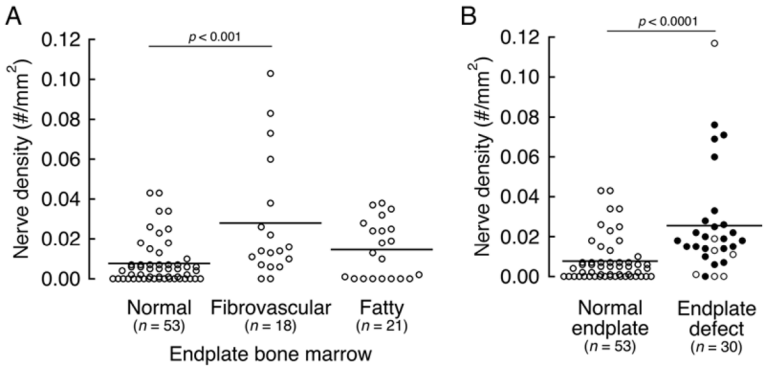

Figure 5.

Comparison of nerve density among endplates with abnormal marrow and between endplates with and without endplate defects (see Methods for classification). **(A)** Abnormal endplate marrow had significantly greater nerve density than did normal endplate marrow ($p < 0.005$, Kruskal-Wallis test). The nerve density in fibrovascular marrow ($p < 0.001$), but not fatty marrow ($p = 0.15$), was significantly higher than that in normal marrow (Mann-Whitney U post-hoc tests). **(B)** The nerve density in and adjacent to endplate defects was significantly greater than that of normal endplates ($p < 0.0001$, Mann-Whitney U test). Note: darkened circles indicate the defected endplates that also contained either fibrovascular or fatty endplate marrow. Horizontal lines indicate group means.

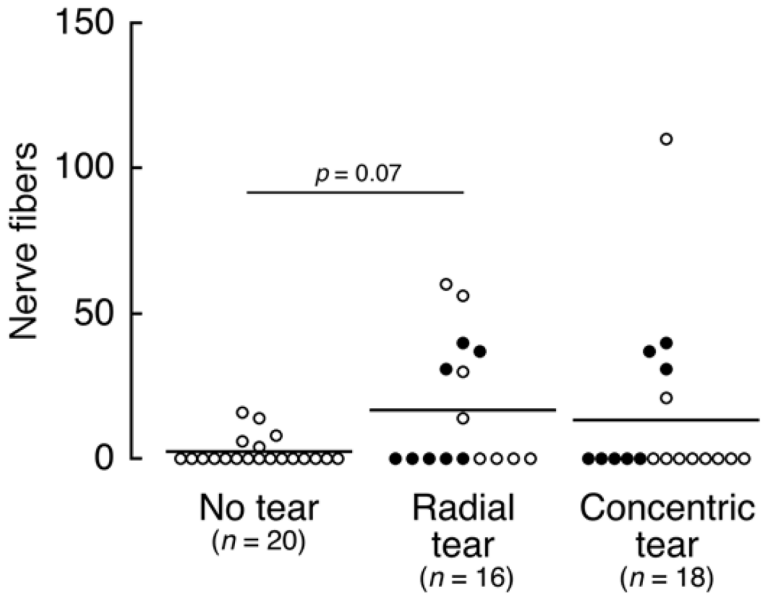

Figure 6.
Comparison of the number of nerve fibers between discs with and without annulus tears. The number of nerve fibers tended to be greater in discs with radial tears than in discs without tears ($p = 0.07$) and was similar between discs with concentric tears and discs with no tears ($p = 0.94$, Mann Whitney U tests). Note: darkened circles indicate discs with both radial and concentric tears. Horizontal lines indicate group means.

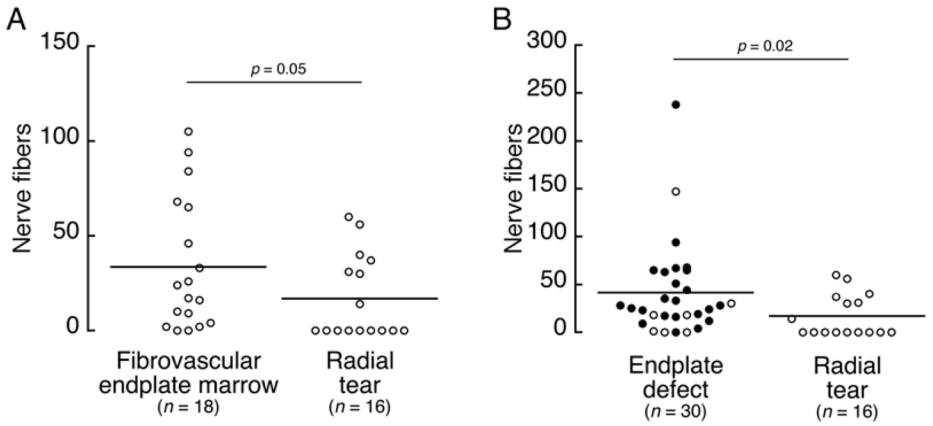

Figure 7.

Comparison of nerve fibers between discs with radial tears and endplates with pathologies. **(A)** The number of nerve fibers was significantly lower in discs with radial tears than in endplates with fibrovascular marrow ($p = 0.05$, Mann-Whitney U test). **(B)** The number of nerve fibers was significantly lower in discs with radial tears than in defected endplates ($p = 0.02$, Mann-Whitney U test). Note: darkened circles indicate the defected endplates that also contained either fibrovascular or fatty endplate marrow. Horizontal lines indicate group means.

Table 1

Incidence, affected anatomical regions, and severity for different types of endplate and disc pathologies

Pathology	Incidence[1]	Affected Region			Severity		
		Anterior	Central	Posterior	Mild	Moderate	Severe
Endplate (n = 92)							
Fibrovascular endplate marrow	19.6% (18)	55.6% (10)	22.2% (4)	22.2% (4)	55.6% (10)	27.8% (5)	16.7% (3)
Fatty endplate marrow	22.8% (21)	47.6% (10)	23.8% (5)	28.6% (6)	33.3% (7)	28.6% (6)	38.1% (8)
Endplate defect	32.6% (30)	46.7% (14)	36.7% (11)	16.6% (5)	23.3% (7)	30.0% (9)	46.7% (14)
Disc (n = 46)							
Radial annular tear	34.8% (16)	43.8% (7)	N/A	56.2% (9)	18.8% (3)	12.5% (2)	68.7% (11)
Concentric annular tear	39.1% (18)	61.1% (11)	N/A	38.9% (7)	55.6% (10)	11.1% (2)	33.3% (6)

[1] Incidence refers to the number of endplates or discs; percentages for region and severity refer to the number of pathologies; N/A – not applicable.